The use of Advanced Numerical Models in The Optimization of Embedding Position of d33 Piezoelectric Transducers

Jamal Najd, Enrico Zappino, Walid Harizi, Erasmo Carrera, Zoheir Aboura

The use of Advanced Numerical Models in The Optimization of Embedding Position of d_{33} Piezoelectric Transducers

Jamal Najd[1,2], Enrico Zappino[1], Walid Harizi[2], Erasmo Carrera[1] and Zoheir Aboura[2]

[1]Mul2 Group, Department of Mechanical and Aerospace Engineering,
Politecnico di Torino, Torino, Italy
Email: jamal.najd@polito.it, enrico.zappino@polito.it
[2]Université de Technologie de Compiègne, Roberval, Compiègne Cedex, France
Email: jamal.najd@utc.fr, walid.harizi@utc.fr

Keywords: Smart Structures, embedded piezoelectric transducers, optimization, plate models, Carrera Unified Formulation (CUF)

Abstract
In this study, the best embedding position of piezoelectric sensors through the thickness of composite materials was investigated for structural health monitoring purposes via Lamb wave propagation. The work encompasses both numerical and experimental approaches towards achieving the desired optimal position. The numerical work utilizes a kinematically refined 2D FE plate model based on the Carrera Unified Formulation, offering a compelling computational cost compared to the full 3D FE models. The numerical results cover a wide scope on the different embedding possibilities whereas the experimental results serve as a qualitative verification.

1. Introduction

Ultrasonic waves have proven effective in detecting damage in both metallic and composite structures [1]. However, the conventional approach involves attaching ultrasonic sensors on the surface, often leading to prolonged downtime for structural servicing, requiring and costing both time and labor. An alternative approach hereby exploited considers utilizing surface-mounted or/and embedded transducers to emit and receive ultrasonic waves, achieving a similar objective without relying on external devices [1,2]. On the other hand, even though composite structures have been adopted widely across major industries such as aerospace, renewable energy, and automotive sectors, the structural health monitoring (SHM) of these structures remains critical and unattainable, with the lack of defined analytical models to detect early damages and prevent potential structural failures. The fabrication process involving laminate by laminate construction allows for the integration of piezoelectric elements within the structures, enabling them to possess sensing/ actuation capabilities[3]. Despite numerous studies focusing on embedded transducers, their embedding and application in industrial settings remains limited due to concerns regarding stress concentration at embedding locations, as well as due to manufacturing difficulties[4].
This study employs advanced multifield two-dimensional finite element models investigating Lamb wave propagation in composite panels to optimize various parameters of sensor/ actuator embedding. Utilizing the Carrera Unified Formulation (CUF) as the basis for the model offers the flexibility to apply varying kinematics at different structural regions. This flexibility allows the use of higher kinematics precisely where sensors and actuators are positioned. Consequently, it becomes possible to describe and alter the through-thickness behavior of composite panels without resorting to cumbersome and computationally expensive three-dimensional models. The focuse here is not on optimizing the

kinematics of the numerical model, but is on exploring various embedding positions within the thickness of the composite panel. The transducers employed in the study are piezoelectric of the normal d_{33} type. Both actuator and sensor positions are examined to determine the optimal embedding positions that enhance actuation and sensing capabilities of fundamental symmetric and antisymmetric Lamb Wave propagation. Evaluation criteria involve assessing the ratio of sensing to actuation potential signal while analyzing the respective modes. Additional experimental results are supplied for the symmetric mode in support of the numerical results, where glass fiber/polyester plates were manufactured with embedded transducers.

2. Numerical Model

The numerical model employed in this study utilizes higher order plate kinematics [5]. As the aim of the study is not to study the model kinematics refinement and impact on the results, but to provide a study case for the different embedding positions, a highly refined layer-wise model was adopted. This model allows for the expression of cubic displacement field at each layer. The model can be derived from the electro-mechanical unknown vector $q = \{u, v, w, \emptyset\}$, where *u*, *v*, and *w* are the unknowns of the displacement components and $\emptyset$ is the unknown of electric potential. For a layer *k*, the N order expansion of the unknown displacement vector q^k can be expressed as: $q^k = F_t q_t^k + F_b q_b^k + F_r q_r^k = F_\tau q_\tau^k$, where $\tau = t, b, r\,; r = 2,3, \dots N, k = 1,2, \dots N_1$. The r-polynomials are introduced for higher order expansions (quadratic, cubic) as in this work and accordingly, the to-the-thickness function $F_\tau(\xi)$ can be written as:

$$F_t = \frac{P_0 + P_1}{2} \qquad F_b = \frac{P_0 - P_1}{2} \qquad F_r = P_r - P_{r-2} \tag{1}$$

Where $P_j = P_j(\xi)$ is the Legendre polynomial of the j-order, with -1< ξ <1, with ξ = -1, 1 denoting the bottom and top of the kth layer. The functions have the following properties to insure the continuity of the unknown vector components at the interfaces between two consecutive elements:

$$\begin{gathered}\text{For } \xi = 1\,, F_t = 1\,, F_b = 0, F_r = 0 \\ \text{For } \xi = -1\,, F_t = 0\,, F_b = 1, F_r = 0\end{gathered} \tag{2}$$

The proposed model is a slender plate with 2/2 twill glass fabrics. The dimensions of the model are shown in **Figure 1**, whereas the mechanical and electrical properties of the host material and piezoelectric transducers used are reported in **Table 1**. The actuator was actuated with an electric potential imposed between the upper and lower surfaces. The shape of the actuation signal in Eqn (3) is a modulated sine wave of frequency f = 200 kHz and a number of oscillations n=10.
The imposed amplitude a was 10V and the model timestep was set to 0.1 μs.

$$\varphi(t) = A\sin(2\pi ft)\sin^2\left(\frac{\pi f\, t}{n}\right) \tag{3}$$

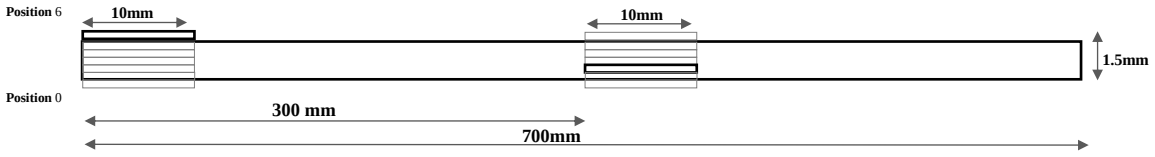

Figure 1. Benchmark with the different possible embedding positions and dimensions

Table 1. Material mechanical and piezoelectric properties

	$E_1=E_2$ (GPa)	E_3 (GPa)	G_{12} (GPa)	$G_{13}=G_{23}$ (GPa)	ν_{12} -	$\nu_{13}=\nu_{23}$ -	ρ kg/m^3
Host material	24.57	10	4.46	4.44	0.13	0.29	1900

	$C_{11}=C_{22}$ (GPa)	C_{33} (GPa)	C_{12} (GPa)	$C_{13}=C_{23}$ (GPa)	$C_{44}=C_{55}$ (GPa)	C_{66} (GPa)	$e_{31}=e_{32}$ (C/m^2)	e_{33} (C/m^2)	X_{33} (nF/m)
PZT material ρ=7750 kg/m^3	120	111	75.2	75.1	21	22.5	-7.8	14.75	7.213

	E (GPa)	ν -	e_{31} (mC/m^2)	e_{32} (mC/m^2)	e_{33} (mC/m^2)	ρ kg/m^3
P(VDF-TRFE)	2.6	0.225	1.44	1.44	-64.34	1900

3. Experimental work

On the other hand, an experimental work was undergone, where piezoelectric ceramic PZT transducers were embedded into 6 plies of 2/2 twill glass fabrics. The plate was manufactured via liquid resin infusion process, where the transducers were embedded according to [1,2]. Three piezoceramic actuators where embedded in the middle of the plate, and four PZT sensors were embedded at different positions through the thickness of the plate to be compared. A schematic and the actual plate can be seen in Figure 2. The plate dimensions are $500\text{mm} \times 500\text{mm} \times 1.5\text{mm}$.

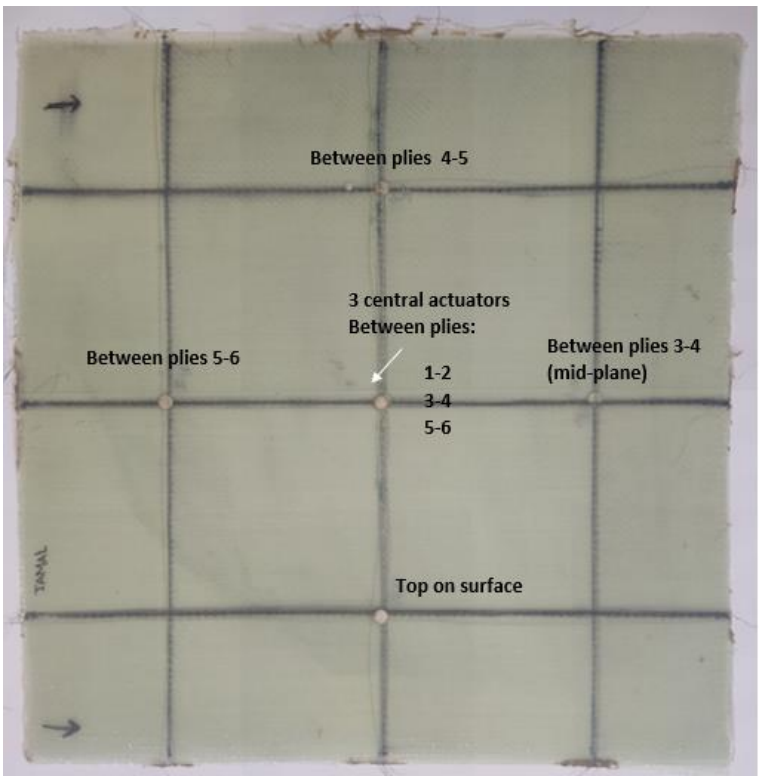

Figure 2. Embedding position of PZT sensors in the manufactured plate

The electric signal of these sensors can be compared as they are embedded in the 2/2 twill fabrics with laminas all with the same orientations, at the 0° and 90° locations and at the same distance from the actuators. The actuators were actuated via a modulated sine wave, of 10 peaks, at a frequency of 200 kHz using a function generator (AFG-3021 -Tektronix - France). The signal at the sensor position was received via an oscilloscope (DSO-X 2002A - Agilent Technologies - USA).

4. Results

For the numerical results, it is worth noting that the in a 2D- matrix of possibilities of embedding sensor and actuator positions, this matrix is symmetric, resulting in similar results, for example for top sensor top actuator and bottom sensor bottom actuator positions. The numerical results were reported in **Figure 3**, where the maximum electric potential for the propagating symmetric and anti-symmetric fundamental lamb waves was plotted.

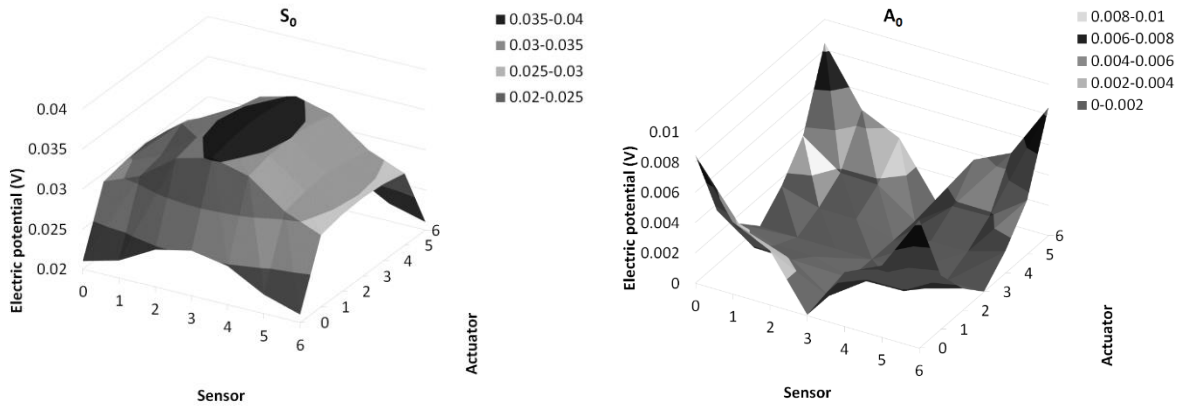

Figure 3. Maximum Electric potential for symmetric (left) and antisymmetric (right) fundamental lamb waves

These results show that the best position to imbed sensors and actuators for symmetric wave is at the middle of the thickness between the plies, whereas the best for antisymmetric waves are surface mounted sensors and actuators. Also, when the actuator is at the middle, the generated antisymmetric lamb wave is negligible, which is understandable, due to the actuation mechanism, and hence, the low electric potential for all sensor positions.

On the other hand, the results of the experimental work were reported in **Figure 4**. For each actuator configuration, the maximum electric potential received at the sensors was plotted. Note that as the symmetric mode is much faster than the antisymmetric one, the reflections of the former mode were captured before the latter mode. Accordingly, only the amplitude of the symmetric lamb wave was reported.

It can be noticed that the highest amplitude for the experimental values lies where the sensor is embedded but near the top, between plies 5-6, among this position, the best was found when the actuator was embedded at the opposite side, between plies 1-2. However, it can also be noticed that the sensor embedding position 3-4 (middle) is the sensor configuration of the second highest amplitude, with actuator position at the middle. The same goes for sensor embedding position 4-5, leaving the lowest amplitude when the sensor is surface mounted, which is expected due to the lower stress concentration around the sensor and less efficiency in converting mechanical motion into electrical signature. These results vary from the numerical ones, especially for the highest values, but that could be explained by the embedding effect, as the embedded sensors are not exactly in the middle, as in the numerical case,

but slightly shifted. Another uncertainty lies in the assumption that the material is homogeneous along the propagation direction. Additionally, the embedding of different actuators at the center could have impacted the local stiffness and thickness highly, as 3 actuators where embedded at that location.

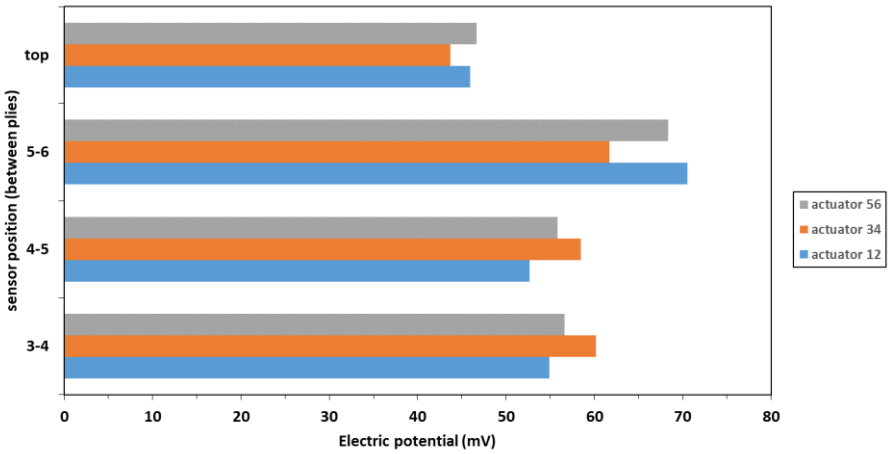

Figure 4. Maximum electric potential in the experimental work for symmetric wave propagation

5. Conclusions

In this work, an introduction about the optimization of the embedding position of actuators and sensors was presented. The approach shows the feasibility to use higher order plate models to gain some aspects about the optimal embedding position, without the use of computationally expensive 3D models. Some experimental results were supplied for embedded PZT, in different locations to shoe the impact on the acquired electrical signal in Lamb wave propagation. Some discrepancy was found for the highest values obtained experimentally, which can be related to possible host material stiffness mismatch in the different directions, and due to embedding effects. A lengthy investigation including the effects of sensor dimensions and embedding positions was recently published [8]. Additional investigation might be required to study the exact embedding effects on the results, while modelling embedded transducers via material removal vs actual embedding with host material undulation.

Acknowledgments

The authors would like to thank the Hauts-de-France Region (France) and Politecnico di Torino (Italy) for the funding of this work as part of the doctoral thesis of Mr. Jamal NAJD (Agreement number 20003877, N GALIS: ALRC2.0-000072). This research was partly funded by the Clean Sky 2 Joint Undertaking under the European Union's Horizon 2020 research and innovation program, Grant Agreement number: 738078—DEsign, development, manufacture, testing and Flight qualification of nExt geNeration fuel storage system with aDvanced intEgRated gauging and self-sealing capabilities (DEFENDER).

References

[1] C. Kralovec and M. Schagerl, “Review of Structural Health Monitoring Methods Regarding a Multi-Sensor Approach for Damage Assessment of Metal and Composite Structures,” *Sensors*, vol. 20, no. 3, 2020, doi: 10.3390/s20030826.

[2] H. Yang *et al.*, “Ultrasonic detection methods for mechanical characterization and damage diagnosis of advanced composite materials: A review,” *Compos. Struct.*, vol. 324, p. 117554,

2023, doi: https://doi.org/10.1016/j.compstruct.2023.117554.

[3] Z. A. C. Tuloup W. Harizi and Y. Meyer, “Integration of piezoelectric transducers (PZT and PVDF) within polymer-matrix composites for structural health monitoring applications: new success and challenges,” *Int. J. Smart Nano Mater.*, vol. 11, no. 4, pp. 343–369, 2020, doi: 10.1080/19475411.2020.1830196.

[4] P. M. Ferreira, M. A. Machado, M. S. Carvalho, and C. Vidal, “Embedded Sensors for Structural Health Monitoring: Methodologies and Applications Review,” *Sensors*, vol. 22, no. 21, 2022, doi: 10.3390/s22218320.

[5] E. Zappino and E. Carrera, “Advanced modeling of embedded piezo-electric transducers for the health-monitoring of layered structures,” *Int. J. Smart Nano Mater.*, 2020, doi: 10.1080/19475411.2020.1841038.

[6] C. Tuloup, W. Harizi, Z. Aboura, and Y. Meyer, “Integration of piezoelectric transducers (PZT and PVDF) within polymer-matrix composites for Structural Health Monitoring applications: new success and challenges.,” *Int. J. Smart Nano Mater.*, no. September, 2020, doi: 10.1080/19475411.2020.1830196.

[7] J. Najd, W. Harizi, Z. Aboura, E. Zappino, and E. Carrera, “Rapid estimation of the fatigue limit of Smart Polymer-Matrix Composites (PMC) using the self-heating tests,” *Compos. Struct.*, no. November, p. 115039, 2021, doi: 10.1016/j.compstruct.2021.115039.

[8] E. C. W. H. Jamal Najd Enrico Zappino and Z. Aboura, “Optimal position and dimensions of embedded normal piezoelectric transducers, higher order plate models and experimental approach,” *Mech. Adv. Mater. Struct.*, vol. 0, no. 0, pp. 1–12, 2024, doi: 10.1080/15376494.2024.2342028.